Spin Polarization in Proton-Xenon Charge-Exchange Collisions*†

R. Shakeshaft‡ and J. Macek
Behlen Laboratory of Physics, University of Nebraska, Lincoln, Nebraska 68508
(Received 13 March 1972)

In a recent paper we briefly reported on the possibility of producing spin-polarized hydrogen atoms through the charge-exchange reaction $H^+ + Xe \rightarrow H(^2S_{1/2}) + Xe^+(^2P_{1/2})$. At proton energies of 15 eV, spin polarization is implied by the preferential population of $Xe^+(^2P_{1/2})$ over $Xe^+(^2P_{3/2})$ and the preliminary two-state calculations presented earlier indicated that a high degree of polarization could be obtained. In this paper we shall give a more complete discussion of the earlier work. In particular we shall describe the model upon which the calculations have been based, and the validity of this model will be examined. Three-state calculations, which allow for the population of $Xe^+(^2P_{3/2})$, have been performed and these results will be compared with the earlier two-state results. We have also calculated the polarization as a function of scattering angle. It is found that the polarization varies rapidly with angle, owing to diffraction effects, and at certain angles almost 100% polarization is achieved.

I. INTRODUCTION

The production of spin-polarized particles continues to be of interest in many branches of physics and many methods have been proposed and employed.[1–4] All methods, except those which depend on weak-interaction decays (which violate parity conservation), achieve spin polarization through the coupling of the spin vector of the particle to an axial vector whose direction is determined by the physical geometry of the experiment. For example, in a Stern-Gerlach experiment the spin of the particle is coupled to an external magnetic field, whereas in the Mott scattering[1] of electrons from gold nuclei the electron spin is coupled to its own orbital angular momentum. In another method, proposed by Fano,[3] electrons are produced spin polarized through photon absorption. Here the electron spin is indirectly coupled to the circular-polarization vector of electromagnetic radiation.

The Fano effect is particularly interesting because it relies on a "leverage" mechanism[5] to amplify the influence of the weak spin-orbit force. We have recently pointed out[4] another leverage mechanism which acts in charge-exchange collisions to produce spin-polarized particles. This latter effect deserves further investigation because of the insight it can provide on the dynamics of atomic collisions. It may also provide a practical method for producing spin-polarized particles. In the case of neutral atoms, such a method would be superior to the Stern-Gerlach experiment which requires a magnetic field and is unsuitable for producing fast spin-polarized atoms. In this paper then, we shall give a more complete discussion of the work reported in Ref. 4.

Our attention is confined to the particular reaction

$$H^+ + Xe \rightarrow H(^2S_{1/2}) + Xe^+(^2P_{1/2}) , \tag{1}$$

in which the incoming proton captures an electron to form hydrogen in its ground state, leaving the xenon ion in its first excited state. This appears to be the simplest system for which spin polarization is likely to occur. The reaction is almost resonant, the energy defect being only 0.17 eV, whereas the energy defect for leaving Xe^+ in the ground state (that is, the $^2P_{3/2}$ state) is 1.47 eV, more than eight times as great, and the energy defect for any other transition is more than 8 eV. One can estimate the proton energies at which transitions to $Xe^+(^2P_{3/2})$ will be important by using Massey's adiabatic principle.[6] This principle states that the cross section for a particular transition is appreciable only when the velocity v of the incident proton satisfies the condition

$$v = a\Delta E/\hbar , \tag{2}$$

where a is the "adiabatic parameter," a length of the order of the atomic dimensions involved, and ΔE is the energy defect associated with the transition. Taking a to be 5 a.u. we find that population of $Xe^+(^2P_{3/2})$ will not become appreciable until proton energies of about 1.8 keV, whereas population of $Xe^+(^2P_{1/2})$ is greatest for energies near 25 eV. Evidently then, in this latter energy range, the effect of the relatively weak spin-orbit interaction is greatly amplified under the leverage implied by the adiabatic principle, which requires a large relative population of $Xe^+(^2P_{1/2})$ over $Xe^+(^2P_{3/2})$. The spin-orbit splitting becomes vital to the outcome of the collision and this strongly suggests that the hydrogen atoms will emerge spin polarized.[7]

This idea vaguely resembles an idea proposed by Schwinger[2] for polarizing fast neutron beams. The scattering of neutrons around 1 MeV from He^4 may be described in terms of a broad $J = \frac{3}{2}$ resonance corresponding to the ground state of He^5; the $J = \frac{1}{2}$ state is at least 2 MeV higher in

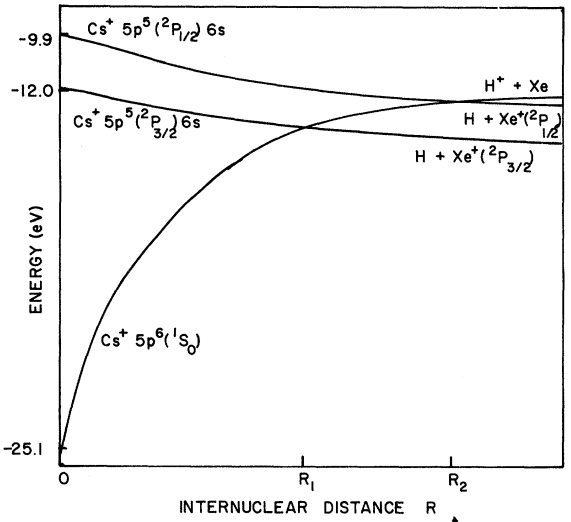

FIG. 1. Estimated diabatic curves for the important states. The vertical scale represents the independent-electron energy.

energy and calculations have shown that the neutrons may be highly polarized as a result of the interference between the scattering from this split resonance and the potential scattering of the s wave. The analogy between Schwinger's method and the method proposed here lies in the fact that the scattering of the unpolarized incident beam depends strongly on the spin-orbit splitting of two levels.

In reaction (1) the orbital angular momentum of the incoming proton provides the axial vector to which the spin of the active electron is (indirectly) coupled. Thus, the orbital angular momentum of the proton is coupled to the orbital angular momenta of the electrons through the interaction potential. The orbital and spin angular momenta of the electrons are in turn coupled through the spin-orbit interaction. Hence, an exchange of orbital angular momentum between the proton and the electron distribution influences the spin state of each electron. This will be shown explicitly in Sec. II.

We have formulated the impact-parameter approximation to include the spin of the electrons and we have obtained a set of coupled differential equations similar in form to those derived by Wilets and Gallaher[8] for the proton-hydrogen system. The mathematical details of this formulation have been presented elsewhere.[9] Preliminary two-state calculations, which were based on the separated atom wave functions and did not allow for intermediate population of $Xe^+(^2P_{3/2})$, were reported earlier[4] and indicated that for protons incident at 15 eV spin polarization occurred to a significant degree. The inclusion of only two states into the calculations can be justified for large impact parameters by the rough sketch of the diabatic curves shown in Fig. 1. In the molecular picture, which is appropriate at low proton energies, the adiabatic curves govern the collision and the chance of a transition is highest in the region of a pseudocrossing between these curves. Referring to Fig. 1, we see that the diabatic state $H+Xe^+(^2P_{3/2})$ will not influence the relevant adiabatic curves in the region of the pseudocrossing at R_2. Hence, for impact parameters greater than and near to R_2, the two-state approximation should be quite adequate, at least for the determination of total cross sections. For impact parameters near R_1 and below we must take account of virtual transitions to $H+Xe^+(^2P_{3/2})$, but we believe virtual transitions to further states to be much less important since they lie much higher in energy.

On the basis of angular-momentum-coupling rules, there are four final channels into which reaction (1) may proceed. However, it will be shown in Sec. II that an important selection rule, arising from reflection symmetry in the scattering plane, rules out two of these channels and also implies that spin polarization cannot be obtained along the beam axis. Certain intermediate channels are also forbidden by this selection rule. Thus, if we allow for intermediate population of the ground state of Xe^+ we need only consider an additional four (rather than nine) channels.

The outline of this paper is as follows. In Sec. II, we shall discuss the symmetry requirements and derive an expression for the polarization fraction in terms of the scattering amplitudes appropriate to reaction (1). In Sec. III, we discuss the impact-parameter approximation and we define the scattering matrix in this approximation. In Sec. IV, we discuss the theoretical model and examine its validity, and in Sec. V, we discuss some aspects of the numerical analysis involved in our calculations. Finally, in Sec. VI, we present the results of two- and three-state calculations performed for protons incident at 15 eV. The scattering amplitudes, and hence the polarization fraction, are obtained first as functions of the impact parameter. However, for practical purposes, we need to know the polarization fraction as a function of scattering angle. This is accomplished using the method of Wilets and Wallace[10] where one performs a Fraunhofer integration over the amplitudes. We have done this and the results will also be given in Sec. VI. It is found that the polarization fraction oscillates very rapidly with the scattering angle and this is explained by strong diffraction occurring in the scattering.

II. SPIN-POLARIZATION THEORY

To describe the collision we choose a fixed orthogonal right-handed set of axes (xyz) orientated

so that the beam of protons is incident along the x axis and scatters into the xy plane. The z axis is therefore perpendicular to the scattering plane. It is helpful to view the two collision partners as two elementary particles, specified by their internal quantum numbers, which interact and exchange an electron via reaction (1). In the final state of the system the total internal angular momentum[11] J may take on the values 0 or 1, on the basis of angular-momentum-coupling rules. However, the Hamiltonian is invariant under a reflection of the internal coordinates in the scattering plane and this leads to a selection rule which precludes J from taking the value zero. To demonstrate this, we introduce the internal reflection operator[12]

$$\mathcal{R}_z = \eta e^{-i\pi \mathcal{J}_z} \mathcal{P} \quad , \tag{3}$$

where $\mathcal{P}$ is the internal parity operator. We can take the phase factor η to be unity if reflections $\mathcal{R}_x$ and $\mathcal{R}_y$ in the yz and xz planes, respectively, are consistently defined by

$$\mathcal{R}_x = e^{-i\pi \mathcal{J}_x} \mathcal{P}, \quad \mathcal{R}_y = e^{-i\pi \mathcal{J}_y} \mathcal{P} \tag{4}$$

Then, if $|JM\rangle$ denotes an eigenstate of $\mathcal{J}^2$ and its projection along the z axis,

$$\mathcal{R}_z |JM\rangle = (-1)^{-M+P} |JM\rangle \ , \tag{5}$$

and hence reflection symmetry gives rise to the conserved dichotomic quantum number $\Gamma = (-1)^{-M+P}$. Here P is the product of the internal parities of the two atomic particles. In the initial state of the system J equals zero, P is even, and there is only one incoming channel, with Γ fixed to be $+1$. In the final state P is odd and since Γ is conserved M must be odd also. Hence M must equal ± 1, so that $J = 0$ is ruled out, and there are just two outgoing channels. In either channel the internal angular momenta of Xe^+ and H are both aligned in the same direction and, if $a_\pm$ are the final-state amplitudes corresponding to $M = \pm 1$, the hydrogen atom is spin polarized along the z axis (and the xenon ion is *angular momentum* polarized to the same degree) provided the quantity

$$P_s = (|a_1|^2 - |a_{-1}|^2)/(|a_1|^2 + |a_{-1}|^2) \tag{6}$$

is nonzero. There is no additional symmetry which might require $|a_{+1}|$ to equal $|a_{-1}|$ and we can assert without further calculation that the hydrogen atom is spin polarized along the axis perpendicular to the scattering plane. The polarization is, in fact, greatest along this axis. For let us take a new set of axes $(x'y'z')$ related to the old set (xyz) by the Euler angles[13] α, β, and γ. Then if a'_M (where M runs over the values -1, 0, and 1) denote the amplitudes referred to the new frame, the polarization fraction P'_s along the z' axis is given by

$$P'_s = (|a'_1|^2 - |a'_{-1}|^2)/I \ , \tag{7}$$

where the intensity $I = |a_1|^2 + |a_{-1}|^2$. The amplitudes a'_M are simply related to $a_{\pm 1}$ by the rotation matrices $D_{M'M}(\alpha\beta\gamma)$ and we can express P'_s in the form

$$P'_s = \frac{|pa_1|^2 + |qa_{-1}|^2 - |qa_1|^2 - |pa_{-1}|^2}{I} \ , \tag{8}$$

where $p = D_{11}(\alpha\beta\gamma)$ and $q = D_{1-1}(\alpha\beta\gamma)$. This expression shows that P'_s vanishes when $\beta = \frac{1}{2}\pi$. That is, no spin polarization can be obtained along an axis lying in the scattering plane and this is easily seen to be a consequence of reflection symmetry. By differentiating the right-hand side of (8) with respect to β, we can verify that P'_s is maximum when $\beta = 0$ and hence that the polarization is maximum along the z axis, the axis perpendicular to the scattering plane. For the rest of this paper we shall only consider the polarization along this latter axis.

Before the collision takes place, the internal orbital angular momentum L of the electron distribution is zero but finally L equals 1, so that the proton must transfer some of its orbital angular momentum to the electrons. We shall now see how this influences the spin of the hydrogen atom. Let M_L be the projection of L along the z axis. Then after the collision M_L may assume the values ± 1 or 0. Now if M_L is zero the spin of the hydrogen atom is as likely to be aligned as antialigned along the z axis. However, if M_L is nonzero the spin of the hydrogen atom is aligned or antialigned along the z axis according to whether $M_L = +1$ or -1. These results follow because the xenon ion is in the $^2P_{1/2}$ state and because reflection symmetry implies $M = \pm 1$. Now exchange to the state $M_L = +1$ will not occur with equal probability to the state $M_L = -1$. Hence the hydrogen atoms must emerge spin polarized. The polarization actually depends on how the proton transfers its orbital angular momentum to the electrons. Although we have introduced reflection symmetry into this argument, it must be stressed that this is merely a simplifying feature and the only condition actually needed to imply polarization is that the xenon ion is preferentially populated in either the $^2P_{1/2}$ or the $^2P_{3/2}$ state.

It is often more convenient to use amplitudes which refer to the beam axis as quantization axis. In this case we use a set of axes $(x'y'z')$ orientated so that the beam is incident along the z' axis and scatters into the $x'z'$ plane. This new set is related to the old set (xyz) by the Euler angles $\alpha = 0$, $\beta = \frac{1}{2}\pi$, and $\gamma = \frac{1}{2}\pi$. In terms of the new amplitudes, b_M say, where M now denotes the projection of the total internal angular momentum along the beam axis, P_s may be expressed in the form

$$P_s = \sqrt{8}\,|b_0 b_1| \sin\Delta / I\,, \tag{9}$$

where Δ is the phase difference between b_0 and b_1. Note that $|b_{-1}|$ equals $|b_1|$ and that, in the linear trajectory approximation, b_1 would be zero if the projection of the internal angular momentum along the internuclear axis were conserved. It has been demonstrated elsewhere[9] that such a conservation rule does not even approximately hold but it is clear from Eq. (9) that should b_1 vanish, no polarization would be obtained.

We have assumed throughout this section that only the $^2P_{1/2}$ state of Xe^+ is populated after the collision. Our three-state calculations bear out this assumption for proton energies of about 15 eV. At much higher energies the $^2P_{3/2}$ state of Xe^+ will also be populated after the collision and the final amplitudes pertaining to transitions to this state will be nonzero, so that the formulas (6) and (9) for the polarization fraction take a more complicated form. The generalization of these formulas is not difficult and need not be dealt with here.

III. IMPACT-PARAMETER APPROXIMATION

In the impact-parameter approximation the two collision partners A and B follow classical paths which we shall assume here to be linear, an assumption which is justified provided the interaction potential between the two particles is much less than their kinetic energy. The internuclear nuclear coordinate $\vec{R}$ may then be written in the form

$$\vec{R} = \vec{\rho} + \vec{v}\,t\,, \tag{10}$$

where $\vec{\rho}$ is the impact parameter and $\vec{v}$ is the velocity of relative motion. The electron wave function Ψ is determined by the Schrödinger equation

$$i\,\frac{\partial \Psi}{\partial t} = \mathcal{H}\Psi\,, \tag{11}$$

where the Hamiltonian $\mathcal{H}$ depends on the time t through $\vec{R}$.

To solve Eq. (11) we expand Ψ in terms of the wave functions ψ_n of the separated atomic system. These functions are assumed to be exact solutions to (11) in the separated atom limit, and they therefore include the translational factors introduced by Bates and McCarroll.[14] The subscript n denotes the quantum numbers J, M, Γ, and P and also further quantum numbers needed to specify the configurations of the two atoms. Writing

$$\Psi = \mathcal{A}\sum a_n \psi_n\,, \tag{12}$$

where $\mathcal{A}$ is the antisymmetrization operator, and substituting this expression into (2), leads to the set of coupled equations

$$i\,\underline{N}\,\dot{\underline{A}} = \underline{M}\,\underline{A}\,, \tag{13}$$

where

$$N_{mn} = \langle \psi_m | \mathcal{A}^\dagger \mathcal{A} | \psi_n \rangle\,, \tag{14}$$

$$M_{mn} = \langle \psi_m | \mathcal{A}^\dagger \left(\mathcal{H} - i\,\frac{\partial}{\partial t}\right) \mathcal{A} | \psi_n \rangle\,, \tag{15}$$

and $\underline{A}$ is a column matrix with the expansion coefficients a_n as elements.

The fixed coordinate frames defined in Sec. II simplified the discussion of spin polarization. However, in any calculation it is most convenient to employ a rotating set of axes, with origin at the centre of mass of the nuclei, orientated so that the quantization axis coincides with the internuclear axis. To be precise, we first define a fixed set of axes $(\hat{\rho}, \hat{n}, \hat{v})$ where the vector $\hat{n} = \hat{v} \times \hat{\rho}$ points out of scattering plane. The rotating set is then defined with respect to this fixed set by the Euler angles $\alpha = 0$, $\beta = \theta$, and $\gamma = 0$, where $\theta = \tan^{-1}[\rho/vt]$. It can be shown[9] that in the rotating frame the elements of $\underline{M}$ take the form

$$M_{mn} = \langle \psi_m | \mathcal{A}^\dagger (V_{AB} - \dot{\theta}\,\mathcal{J}_{\hat{n}}) \mathcal{A} | \psi_n \rangle\,, \tag{16}$$

where V_{AB} is the interaction between particles A and B when the system is in the state ψ_n and $\mathcal{J}_{\hat{n}}$ is the projection of the internal angular momentum operator along the axis perpendicular to the scattering plane. Note that both the spin and space parts of ψ_n are quantized along the internuclear axis. The term $\dot{\theta}\mathcal{J}_{\hat{n}}$ is the semiclassical limit of $\vec{L}_R \cdot \vec{J}/mR^2$, where $\vec{L}_R$ is the orbital angular momentum of the relative motion of A and B, $\vec{J}$ is of course the sum of the internal angular momenta of A and B, and m is the reduced mass of the system. Thus $\dot{\theta}\mathcal{J}_{\hat{n}}$ describes the rotational coupling of the orbital angular momentum of relative motion with the internal electron angular momentum. This term induces transitions between states having different total magnetic quantum number.

Let us suppose that initially, at time $t = -\infty$, the system is in the state specified by ψ_k. The coupled differential equations (13) are then solved subject to the boundary condition

$$\lim a_n = \delta_{nk} \quad \text{as } t \to -\infty \tag{17}$$

and the scattering matrix $\underline{S}$ is defined by the relation

$$S_{nk} = \lim a_n \quad \text{as } t \to \infty\,. \tag{18}$$

Unitarity and time-reversal invariance impose certain conditions on the scattering matrix which provide invaluable checks on the programming and numerical analysis of the calculations. These conditions have been derived elsewhere[15] and will simply be stated here: Unitarity implies that

$$\underline{S}^\dagger\,\underline{S} = I \tag{19}$$

and time-reversal invariance implies that

$$S_{n_1 n_2} = (-1)^{M_1+M_2+P_1+P_2} S_{n_2 n_1} \quad . \tag{20}$$

IV. THEORETICAL MODEL

A. Description of Model

In forming a reliable model upon which the calculations are to be based, we are guided by two criteria. First, it is clear from the adiabatic principle that accurate binding energies must be used since the cross section for a particular transition depends crucially on the energy defect. Second, since the collision is governed by the adiabatic curves accurate wave functions and potentials must be used. The first requirement can be met by employing the experimental binding energies. The second requirement is more difficult to satisfy since the only wave functions available for xenon are those tabulated by Herman and Skillman.[16] The self-consistent-field calculation from which these wave functions are obtained (along with the single-particle potential) predicts an ionization energy of 11.38 eV compared with the experimental ionization energy of 12.13 eV for the atom. The error of 6% in the approximate ionization energy gives some idea of the accuracy of the Herman-Skillman wave functions and potential.

In constructing the Hamiltonian for the complete system we shall ignore the inner-shell and subshell electrons of xenon. These electrons are tightly bound[17] and we will assume that they do not participate in the collision when the proton is incident at a large impact parameter. Thus we shall only consider impact parameters greater than 6 a.u. In the outermost subshell of the atom there are six $5p$ electrons, one of which is the active electron, the remaining five being the spectators. We shall antisymmetrize over all six electrons. In the independent-particle approximation the Hamiltonian has the form

$$\mathcal{H} = \mathcal{K} + \sum_{i=1}^{6} \left(U(r_{ia}) + \beta(r_{ia})\, \vec{L}_{ia} \cdot \vec{S}_{ia} - \frac{1}{r_{ib}} \right) + \frac{6}{R} \quad , \tag{21}$$

where the subscripts a and b refer to the xenon nucleus and the incident proton, respectively. Here $\mathcal{K}$ is the kinetic-energy operator for the complete system, U is the Herman-Skillman single-particle potential for xenon, and the spin-orbit term $\vec{L}_{ia} \cdot \vec{S}_{ia}$ is understood to be an operator with coefficient

$$\beta(r_{ia}) = -\frac{1}{2c^2} \frac{1}{r_{ia}} \frac{dU}{dr_{ia}} \quad . \tag{22}$$

The effect of this operator is accounted for by the experimental binding energies. We have assumed that the active electron moves in the same potential as the spectator electrons and we have neglected relaxation of the spectators as the active electron is removed from the xenon atom. Consistent with these approximations, we have used the same single-particle wave functions for Xe^+ as we have for Xe. The effective charge that the spectator electrons see near the nucleus should not change much after the active electron has been removed, but far away from the nucleus the charge that a spectator electron sees must change from + 1 to + 2. Hence the asymptotic part of the Xe^+ wave function is incorrectly represented. The discrepancy can be estimated from the well-known solution of the Schrödinger equation for the pure Coulomb potential which predicts that the asymptotic radial wave function for a modified Coulomb potential (which tends to a pure Coulomb potential at large r) should be

$$c r^{1/(2E)^{1/2}} e^{-(2E)^{1/2} r} / r \quad , \tag{23}$$

where c is a constant that may be determined by using effective range theory and E is the binding energy of the electron in atomic units. The ionization energy of Xe is about 0.5 a.u. and of Xe^+ about 0.75 a.u. Hence we are representing the proper asymptotic form $cr^{1/5} e^{-1.2r}$ for the radial wave function of Xe^+ by ce^{-r}.

The interaction between Xe and H^+ is

$$\frac{6}{R} - \sum_{i=1}^{6} \frac{1}{r_{ib}} \quad , \tag{24}$$

and the interaction between Xe^+ and H is

$$U(r_{6a}) + \beta(r_{6a})\, \vec{L}_{6a} \cdot \vec{S}_{6a} - \sum_{i=1}^{5} \frac{1}{r_{ib}} + \frac{6}{R} \tag{25}$$

if we denote the active electron by the sixth one. In evaluating $\underline{M}$ the spin-orbit term in (25) will, of course, appear in both direct and coupling single-particle matrix elements. In the direct elements this term appears between hydrogen wave functions, whereas in the coupling elements it appears between a $5p$ xenon wave function and a hydrogen wave function. The coupling matrix element will be small since $\beta(r_{6a})$ is large only for small r_{6a} and the oscillations in the xenon radial wave function cancel the contribution in this region. The direct matrix element will also be small if the internuclear separation is large since the hydrogen atom is then far from the xenon nucleus. Hence, at large impact parameters the interaction between the spin of the outgoing hydrogen atom and its orbital angular momentum about the xenon nucleus is not important, and we have not included this interaction in our calculations.

To some extent, the distortion of the xenon atom under the influence of the incoming proton has been included in our model by allowing for charge exchange.[18] However, the charge-ex-

change interaction decays exponentially with R, whereas the actual interaction between the proton and atom tends at large R to $-\alpha/R^4$, where α is the polarizability of xenon. This latter interaction arises from the virtual excitation of xenon and can be properly accounted for only by including some of the excited states of the atom into the calculations, a formidable task which we have assumed to be unnecessary. We should note, however, that because the adiabatic curves for $H^+ + Xe$ and $H + Xe^+(^2P_{1/2})$ are so narrowly separated at large R, the excited states of xenon may significantly shift the pseudocrossing between these two curves. Nevertheless, we have calculated that the term α/R^4 is a factor of 10 less than the molecular coupling between $H^+ + Xe$ and $H + Xe^+$ $(^2P_{1/2})$ and for this reason the general shape of the adiabatic curves will not be altered by including more states of xenon.

B. Summary of Approximations

There are eight approximations: (i) the linear trajectory approximation; (ii) the approximation that the center of mass of the system is at the xenon nucleus; (iii) the neglect of the inner shells of xenon; (iv) the independent-particle approximation; (v) the use of approximate wave functions and potentials; (vi) the neglect of the relaxation of the spectator electrons of xenon as the active electron is removed; (vii) the neglect of the spin-orbit interaction between Xe^+ and H; and (viii) the inclusion of only two or three states, which do not account for the large induced dipole moment of the xenon atom.

Most of these approximations have been discussed earlier. The use of the linear-trajectory approximation at proton energies of 15 eV is assumed to be valid for impact parameters greater than 6 a.u., where the average potential is weak. In approximation (ii) we have taken the center of mass of the system to be at the xenon nucleus since the xenon atom is 131 times heavier than the hydrogen atom. Approximation (iii) needs further discussion. The active electron cannot penetrate the inner shells of the target because of the Pauli exclusion principle but, since we have ignored these shells in our model, we allow the active electron to move arbitrarily close to the target nucleus after it has been captured by the proton. Now near the target nucleus the captured electron moves in a strong attractive potential leading to a spurious contribution, at small internuclear distances, to the molecular potential of the $H + Xe^+$ system. To eliminate this spurious contribution we must modify the hydrogen wave function so that in the united atom limit it becomes the 6s wave function of Cs^+. Thus, in the united atom limit, the wave function of the captured electron should have five nodes, which minimize the contribution from U inside the inner shells. We have not performed any such modification since for internuclear distances greater than 6 a.u. the hydrogen wave function barely extends into the target. We are confident that, except perhaps for the use of Herman-Skillman xenon wave functions and potentials, all of the approximations listed above are good for impact parameters greater than 6 a.u.

V. NUMERICAL ANALYSIS

A. Charge-Exchange Integrals

The most difficult numerical problem encountered in charge-transfer calculations is the evaluation of integrals involving the overlap of the initial and final wave functions. An ingenious method for solving such integrals has been given by Cheshire.[19] However, Cheshire's method requires analytical wave functions and is inapplicable to the present problem. We shall describe here another method which is most successful for low-energy scattering.

We are required to evaluate the two integrals

$$I_1 = \int F_1(r_a)\, Y_{1m}^*(\hat{r}_a)\, e^{i\vec{v}\cdot\vec{r}_a - \lambda r_b}\ (1/r_b)\, Y_{00}(\hat{r}_b)\, d\vec{r}_a \tag{26}$$

and

$$I_2 = \int F_2(r_a)\, Y_{1m}^*(\hat{r}_a)\, e^{i\vec{v}\cdot\vec{r}_a - \lambda r_b}\, Y_{00}(\hat{r}_b)\, d\vec{r}_a\ , \tag{27}$$

where $\lambda = 1$ and F_1 and F_2 are numerical functions known only at the points of the Herman-Skillman mesh. Replacing F_1 by $-F_2$ in (26) and differentiating I_1 with respect to λ yields I_2 so that is sufficient to determine an algorithm for evaluating I_1.

Integration over the angular coordinates is facilitated by the expansion

$$e^{i\vec{v}\cdot\vec{r}_a - \lambda r_b}\,\frac{1}{r_b}\,Y_{00}(\hat{r}_b) = Y_{00}(\hat{r}_a)\sum_{ll'm'} a_{ll'm'} \times f_l(r_a, R)\, j_{l'}(vr_a)\, Y_{l0}(\hat{r}_a)\, Y_{l'm'}(\hat{r}_a)\ , \tag{28}$$

in which we have used the multipole expansion of $e^{iv\vec{r}}$ and the well-known expansion of the Green's function $e^{-\lambda r_{12}}/r_{12}$.[20] Here we have

$$a_{ll'm'} = 4\pi[4\pi(2l+1)]^{1/2}(i)^{l'}\, Y_{l'm'}^*(\hat{v}) \tag{29}$$

and

$$f_l(r_a, R) = -\lambda j_l(i\lambda r_<) h_l^{(1)}(i\lambda r_>)\ , \tag{30}$$

where

$$r_< = \min(r_a, R),\quad r_> = \max(r_a, R)\ , \tag{31}$$

j_l is the spherical Bessel function, and $h_l^{(1)}$ is the spherical Hankel function of the first kind. Performing the angular integration we obtain

$$I_1 = \sum_{ll'} b_{ll'} C(l'l1; m0m)\, C(l'l1; 000)\, G_{ll'}\ , \tag{32}$$

where we have used the notation of Rose[21] for the

Clebsch-Gordan coefficients $C(l_1 l_2 l_3;\ m_1 m_2 m_3)$ and where

$$b_{ll'} = 4(2l+1)\,(i)^{l'}\,[\pi(2l'+1)/3]^{1/2}\,Y^{*}_{l',m}(\hat{v}) \qquad (33)$$

and

$$G_{ll'} = \int_0^\infty F_1(r) f_l(r,R) j_{l'}(vr)\, r^2 dr\ . \qquad (34)$$

The integrals $G_{ll'}$ are evaluated by some standard numerical procedure.

The triangular property of the Clebsch-Gordan coefficients means that only terms where $l = l' \pm 1$ will contribute to the sum in (32). Now if v is small $G_{ll'}$ tends to zero very rapidly as l' becomes large. This may be seen roughly as follows. For large r, $|f_l j_{l'}|$ is small and since F_1 decays exponentially with r the integrand in (34) is effectively cut off after a distance r_0, where r_0 may be chosen independent of l and l'. Now $|F_1 f_l|$ is bounded by some B which is also independent of l and l' and

$$|j_{l'}(x)| < \tfrac{1}{2}\pi^{1/2}(\tfrac{1}{2}x)^{l'}/\Gamma(l'+\tfrac{3}{2})\ . \qquad (35)$$

Hence we have

$$|G_{ll'}| < \frac{\pi^{1/2} B r_0^3}{2(l'+3)\,\Gamma(l'+\frac{3}{2})}\left(\frac{v r_0}{2}\right)^{l'}\ , \qquad (36)$$

showing that as l' becomes large $G_{ll'}$ tends to zero for all v and tends rapidly to zero if v is small. It can be shown that the series (32) converges for all v. For v equal to 0.2 a.u. we found that it was necessary to sum only the terms $l' \leq 2$ in the series to gain at least three-place accuracy in I_1.

B. Inversion of Normalization Matrix

In solving the coupled differential equations (13), the complex matrix $\underline{N}$ must be inverted at each integration step. The straightforward inversion of $\underline{N}$ at each step is very time consuming and instead we employed an iterative method, suggested by Lipsky,[22] which was found to be much faster. Let $\{t_k\}$ denote the (unequally spaced) mesh of time points over which the equations are integrated, and let $\underline{N}_k$ denote $\underline{N}(t_k)$. We have

$$\underline{N}_{k+1} = (\underline{I} + \underline{C}_k)\,\underline{N}_k\ , \qquad (37)$$

where

$$\underline{C}_k = (\underline{N}_{k+1} - \underline{N}_k)\,\underline{N}_k^{-1}\ , \qquad (38)$$

and hence

$$\underline{N}_{k+1}^{-1} = \underline{N}_k^{-1}\,(\underline{I} + \underline{C}_k)^{-1} \qquad (39)$$

$$= \underline{N}_k^{-1} \sum_{j=0}^{\infty} (-\underline{C}_k)^j\ . \qquad (40)$$

Thus, knowing $\underline{N}_k^{-1}$ we can determine $\underline{N}_{k+1}^{-1}$. However, $\underline{N}_0 = I$ so that we do not have to perform a single inversion. The diagonal elements of $\underline{C}_k$ are of order $h_k = v(t_{k+1} - t_k)$ and the off-diagonal elements of $\underline{C}_k$ are zero when k corresponds to either the united or separated atom limit and are small at other k. Consequently the power series in (40) converges rapidly and we found it necessary to sum only five terms to gain at least three-place accuracy in the final iteration.

VI. RESULTS AND DISCUSSION

The many-particle matrix elements of $\underline{M}$ and $\underline{N}$ were reduced to expressions in single-particle integrals which were then evaluated numerically. In the two-state approximation there were three coupled differential equations to solve whereas in the three-state approximation there were seven. The integration of these equations was accomplished using the fourth-order Runge-Kutta method and all calculations were performed with the IBM 360/65J machine at the University of Nebraska Computing Center. The unitarity and time-reversal symmetry of the scattering matrix is invalidated in our model by the expression (16) for the matrix $\underline{M}$, which depends on using the energy eigenvalues of the approximate wave functions rather than the experimental energies. Thus, in order to test the calculations, we first used Herman-Skillman energies and after unitarity and time-reversal invariance were confirmed to three place accuracy we replaced the Herman-Skillman energies by the experimental energies. Unitarity no longer holding, we then found that the sum of the direct and charge-transfer probabilities differed from unity by as much as 30% at a given impact parameter. Hence, at each impact parameter, we have renormalized the results by dividing the final amplitudes by a common factor determined to ensure that the sum of the probabilities be unity.

We have calculated total charge-transfer cross sections for proton energies of 15, 300, and 1000 eV and our results agree well with the experimental values measured by Koopman.[23] At 1 keV we find that the $^2P_{1/2}$ and $^2P_{3/2}$ states of Xe^+ are about equally populated and the three-state approximation yields a total charge-transfer cross section of 29×10^{-16} cm^2 compared to the experimental value of 30×10^{-16} cm^2. The cross section remains roughly constant down to 15 eV, rising slightly as the energy decreases in accordance with typical resonance behavior. However, at 15 eV we calculate the population of $Xe^+(^2P_{3/2})$ to be negligible.

In Fig. 2, we present the results of two- and three-state calculations performed for protons incident at 15 eV. We have plotted the spin-polarization fraction P_s as a function of impact parameter ρ. Positive polarization corresponds to the spin of the hydrogen atom aligned along the vector $\vec{k}_i \times \vec{k}_f$, where $\vec{k}_i$ and $\vec{k}_f$ are the initial and final momenta of the projectile. At large ρ, P_s is a slowly varying function of ρ. As ρ is decreased P_s increases steadily to a maximum, $P_s^{\max}$ say,

and then begins to oscillate. This feature persists at all proton energies although P_s^{max} decreases as the energy increases. At 15 eV, P_s^{max} is about 0.75 but drops to about 0.30 at 1 keV. This drop is to be expected since as the energy increases the relative population of the $^2P_{1/2}$ and $^2P_{3/2}$ states becomes smaller and the spin-orbit splitting is not so significant. The sharp variation of the polarization fraction with impact parameter, seen in Fig. 2 below $\rho = 7$ a.u., is typical of phenomena which are sensitive to phase changes.

We have also plotted in Fig. 2 the yield of hydrogen, and this is seen to be considerable even at large ρ. The discrepancy between the two- and three-state calculations is perhaps surprising since the three-state calculations reveal that, for $\rho > 6$ a.u., transitions to $Xe^+(^2P_{3/2})$ occur with a probability less than 10^{-4}. However, it must be remembered that virtual transitions to this state will influence the adiabatic curves and consequently effect the final amplitudes.

A method for calculating differential cross sections, once the amplitudes have been obtained at all impact parameters, has been given by Wilets and Wallace.[10] With the internuclear axis as quantization axis, the differential cross section for a transition into a particular channel with total internal magnetic quantum number M is

$$(k_f/k_i)\,|f_M(\theta)|^2\ , \tag{41}$$

where

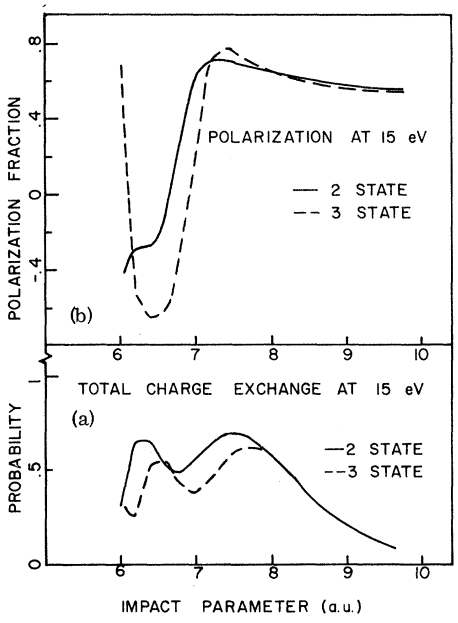

FIG. 2. (a) Probability for producing hydrogen at 15 eV and at impact parameters greater than 7 a. u. (b) Corresponding spin-polarization fraction.

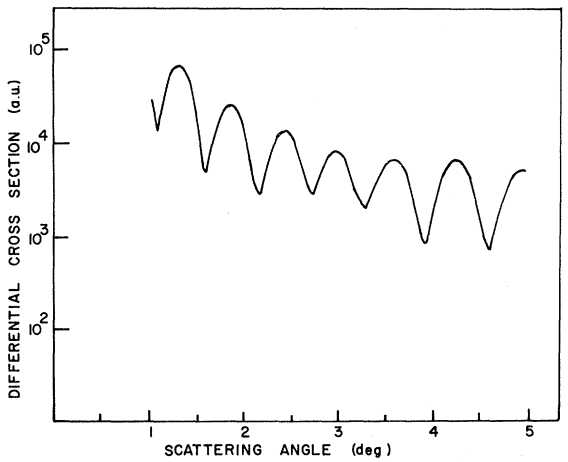

FIG. 3. Differential cross section $d\sigma/d\Omega$ for producing hydrogen at 15 eV between 1° and 5°. We have computed $d\sigma/d\Omega$ from the two-state amplitudes.

$$f_M(\theta) = (-i)^{M+1} k_f \cos^2(\tfrac{1}{2}\theta) \int_0^\infty \rho\, d\rho\, a_M(\rho) \times J_M(k_f \rho \sin\theta)\ , \tag{42}$$

and where θ is the scattering angle and $a_M(\rho)$ is the amplitude, calculated at all impact parameters in the linear-trajectory approximation, pertaining to the transition. At proton energies of 15 eV only the $^2P_{1/2}$ state of Xe^+ will be populated after the collision and there are only two final channels which can be reached. The differential cross section for producing hydrogen is

$$\frac{d\sigma}{d\Omega} = \frac{k_f}{k_i} \sum_M |f_M(\theta)|^2\ , \tag{43}$$

where the sum is over the final total internal magnetic quantum numbers of the system. Since k_f very nearly equals k_i, we can take the factor k_f/k_i to be unity. Note that $|f_{-1}|$ equals $|f_1|$ and that, in analogy with Eq. (9) (recalling that the beam and internuclear axes coincide finally), the polarization fraction is determined by the formula

$$P_s = \frac{(8)^{1/2} |f_0 f_1| \sin\Delta}{(d\sigma/d\Omega)}\ , \tag{44}$$

where Δ is the phase difference between f_0 and f_1.

We have computed $d\sigma/d\Omega$ at 15 eV from the two-state amplitudes and have plotted the results in Fig. 3 for scattering angles between 1° and 5°. In the limit of classical scattering a unique relation is obtained between impact parameter and scattering angle. In this limit we require the phases of the amplitudes $a_M(\rho)$ to change very rapidly with ρ so that the stationary-phase approximation can be applied to the diffraction integral in Eq. (42). Referring to Fig. 3, we see that the differential cross section diminishes with angle

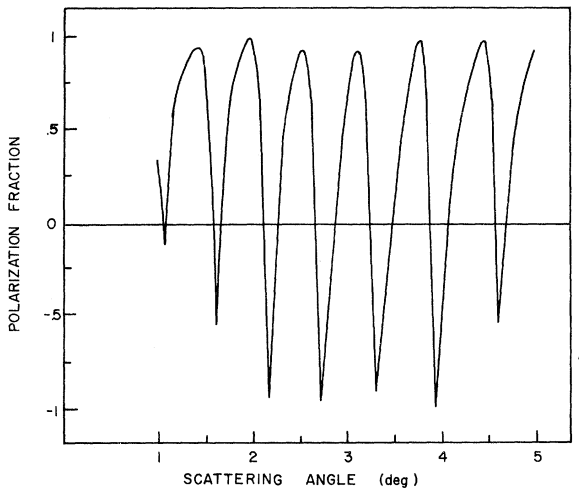

FIG. 4. Polarization fraction, computed from the two-state amplitudes, for hydrogen scattered at 15 eV between 1° and 5°.

but oscillates with a period of about half of a degree. These oscillations are evidently due to diffraction and the scattering is clearly not classical. Hence a unique relation between ρ and θ does not exist. Nevertheless, small-angle scattering should correspond to the range of large impact parameters. Thus we expect that if θ is less than 5° only the region of large ρ will contribute to the integral in Eq. (42). Indeed, no visible difference is noticed in $d\sigma/d\Omega$ by terminating the integration at ρ equal to 4 a.u. instead of zero. This is fortunate because our model, and hence the amplitudes, cannot be trusted at small impact parameters.

Diffraction effects are to be expected in the differential cross sections since the target atom behaves rather like a zone plate (transmitting proton instead of light waves). Considering only those protons which capture an electron, the probability that the target will transmit a proton incident at a given impact parameter is shown in Fig. 2. Instead of being a step function, as in a zone plate, the transmission probability is a smooth function of ρ. Actually at 15 eV charge exchange occurs mostly at impact parameters greater than 6 a.u. and, as far as charge exchange is concerned, it is more appropriate to regard the target atom as a completely opaque disk of radius 6 a.u. having a partially transparent outer edge, the transparency decaying exponentially with radius. In the small-angle scattering of light from such a disk, diffraction minima occur at angles separated by

$$\Delta\theta = \tfrac{1}{12}\lambda \text{ rad}, \tag{45}$$

where λ is the wavelength of the light. The wavelength of 15-eV protons is about 0.12 a.u. and hence we expect diffraction minima to occur in the charge-exchange scattering at angles separated by about $\frac{1}{2}°$, in good agreement with the results.

In Fig. 4, we have plotted the polarization as a function of angle. Since the small-angle scattering occurs in the region of large impact parameters, and since the polarization is positive and slowly varying at large impact parameters, we would expect the polarization to be positive and slowly varying for scattering angles less than 5°. However, diffraction effects produce deep and sharp minima in the polarization fraction and these minima correspond exactly to the diffraction minima of $d\sigma/d\Omega$. It is clear that the average value of the polarization over the range 1°–5° is what we would expect from Fig. 2 in the absence of diffraction. However, at certain angles almost 100% polarization may be achieved, showing that diffraction effects enhance spin polarization to a marked degree.

VII. CONCLUSION

In this paper we have attempted to show that highly spin-polarized atoms may emerge from charge-exchange collisions. We have studied the simplest system in which spin polarization is likely to occur and, from calculations based on a simple model, we have predicted that 100% spin polarization can be attained. Although it is difficult to estimate the error of our calculations, it seems reasonable to expect that the general features of our results are correct. Thus, although a more refined calculation of the polarization (as a function of scattering angle) may alter the positions of the diffraction minima, the existence of these minima and the attainment of 100% polarization at certain angles is likely to remain valid.

The diffraction minima are fairly well separated and the angular resolutions in present-day experiments are easily sufficient for proton-xenon charge exchange to be a practical method of producing spin-polarized hydrogen atoms. Spin-polarized muonium could also be produced by using muons instead of protons and it is feasible to expect that, by choosing the appropriate reaction, a large variety of spin-polarized ions and atoms could be produced through charge-exchange collisions.

ACKNOWLEDGMENT

We are most grateful to Dr. L. Lipsky for many helpful conversations on the numerical aspects of the calculations.

*Based in part on a Ph. D. thesis submitted to the University of Nebraska by R. S.

†Supported in part by the National Science Foundation.

‡Present address: Physics Department, New York University, 4 Washington Place, New York, N. Y. 10003.

[1]J. Kessler, Rev. Mod. Phys. 41, 3 (1969).

[2]L. Wolfenstein, Ann. Rev. Nucl. Sci. 6, 43 (1956).
[3]U. Fano, Phys. Rev. 178, 131 (1969).
[4]J. Macek and R. Shakeshaft, Phys. Rev. Letters 27, 1487 (1971).
[5]In this connection see the note by U. Fano, Comm. At. Mol. Phys. 2, 36 (1970).
[6]H. S. W. Massey and E. H. S. Burhop, *Electronic and Ionic Impact Phenomena* (Oxford U. P., New York, 1952), p. 450.
[7]The hydrogen nuclei are not, of course, spin polarized.
[8]L. Wilets and D. F. Gallaher, Phys. Rev. 147, 13 (1966).
[9]R. Shakeshaft, J. Phys. B 5, 559 (1972).
[10]L. Wilets and S. J. Wallace, Phys. Rev. 169, 84 (1968).
[11]We ignore the nuclear spin, which is assumed to be conserved throughout the collision. Thus J is the sum of the internal *electronic* angular momenta of the two atomic particles.
[12]The form of this operator is obtained by noting that a reflection in the xy plane is equivalent to an inversion in the origin followed by a rotation of π rad about the z axis.
[13]M. E. Rose, *Elementary Theory of Angular Momentum* (Wiley, New York, 1957), Chap. IV.
[14]D. R. Bates and R. McCarroll, Proc. Roy. Soc. (London) A245, 175 (1958).
[15]R. Shakeshaft and J. Macek, J. Phys. B 5, L63 (1972). We are indebted to Professor E. Gerjuoy for pointing out the importance of time-reversal invariance in providing a numerical check.
[16]F. Herman and S. Skillman, *Atomic Structure Calculations* (Prentice-Hall, Englewood Cliffs, N. J., 1963).
[17]The 5s electrons have a binding energy of about 19 eV.
[18]To the same extent we have included the distortion of the outgoing hydrogen atom under the influence of the xenon ion. However, this effect will not be so important since the polarizability of hydrogen is small.
[19]I. M. Cheshire, Proc. Phys. Soc. (London) 92, 862 (1967).
[20]T. Wu and T. Ohmura, *Quantum Theory of Scattering* (Prentice-Hall, Englewood Cliffs, N. J., 1962), p. 43.
[21]Reference 13, Chap. III.
[22]L. Lipsky (private communication).
[23]D. W. Koopman, Phys. Rev. 154, 79 (1967). Koopman has measured total transfer cross sections for proton energies between 70 and 1050 eV.

PHYSICAL REVIEW A VOLUME 6, NUMBER 5 NOVEMBER 1972

Open-Channel Projectors for Rearrangement Processes in Molecular Collisions*

Thomas F. George† and William H. Miller‡
Inorganic Materials Research Division, Lawrence Berkeley Laboratory, and Department of Chemistry, University of California, Berkeley, California 94720
(Received 26 April 1972)

A general form for the projector onto open channels for rearrangement processes in molecular collisions is given. This form is investigated for two special cases of the three-atom process $A+BC \rightarrow AB+C$ on a single potential-energy surface: (a) the rearrangement to and from the ground vibrational and rotational states of BC and AB for arbitrary total angular momentum and (b) the semiclassical limit of this form. The projector for special case (a) can be found exactly under either of two limiting conditions, and for case (b) we find the projector to be a local operator, such that in the semiclassical limit the process $A+BC \rightarrow AB+C$ occurs only when the distance from A to the center of mass of BC equals the distance of C from the center of mass of AB.

I. INTRODUCTION

The unified reaction theory of Feshbach[1] has been applied extensively to problems in nuclear and molecular collisions. The general expressions include an operator P, the projector onto some or all of the open channels and its orthogonal complement $Q=1-P$. Explicit expressions for P can be written formally in a straightforward manner if the collision system involves only elastic or inelastic transitions. For instance, for the inelastic collision of molecules A and B, P can be written as

$$P=\sum_i |\phi_i\rangle\langle\phi_i| , \tag{1.1}$$

where ϕ_i is a product of the internal-state wave functions for each A and B, and the summation runs over all energetically allowed states ϕ_i. P is uniquely defined in this manner to project onto all open channels (corresponding to the states of the system $A+B$ at infinite separation). Q is thus uniquely defined to project onto all closed channels.[2]

The definitions of P and Q for rearrangement collisions in a time-independent theory have presented somewhat of a problem in the past 10 yr. This problem results from the fact that the basis set in one arrangement is not orthogonal to the basis set in another arrangement.[3] A P for rearrangement collisions was first derived by Mittleman[4] and modified by Coz.[5] The complexity of this derivation led Chen and Mittleman[6] to derive simpler expressions for P which, however, did not account in general for possible recoil of the target. Starting with the procedure of Ref. 6,